Available online at www.sciencedirect.com
SCIENCE DIRECT®
Pergamon
Cement and Concrete Research 33 (2003) 1967–1981
CEMENT AND CONCRETE RESEARCH

Physical and mechanical properties of fine hydraulic mixtures

André Lecomte[a,*], Nelly Vulcano-Greullet[a], Claude Steichen[b,1], Guy Scharfe[b,1]

[a]EA 1116 - MMGC, Université Henri Poincaré Nancy 1, IUT de Nancy-Brabois, Département Génie Civil, F-54601 Villers-lès-Nancy, Cedex, France
[b]Laboratoire d'Essai des Matériaux, Ponts et Chaussées du Grand Duché de Luxembourg, 23 rue du Chemin de Fer, L-8005 Bertrange, Luxembourg

Received 23 August 2002; accepted 20 June 2003

Abstract

This two-part article deals with the problem of the fissuring of sandstones reconstituted from fine hydraulic mixtures packed and vacuum dried according to a patented procedure. During more than two years, the dimensional variations of these products were measured on slender test pieces reconstituted according to several models proposed for hydraulic concretes.

In this part, we present the materials, the procedures used to mould the stones along with the calculations developed to obtain the exact composition of the test pieces. We also give densities, the mechanical strength and recorded time evolution of the deformations for different conservation modes which are representative of the possibilities of the envisaged production. In the second part, we present the method for describing the dimensional variations and the adaptations leading to the introduction of a crack index in choice of the formulas.

Keywords: Curing; Drying; Characterization; Physical properties; Shrinkage

1. Introduction

Between the setting and the long term, the hydraulic mixtures undergo various changes in dimension especially linked with the action of water present in the porous material (wetting of the binder, drying, soaking) [1]. Depending on the quality of the product (formula, strength) and on the type of environment (immersion, wrapping, conservation in open air), generally, the induced shrinkages (plastic, thermal, endogenous, drying) give rise to the formation of more or less important cracks at core and/or on the surface of the pieces. Different shrinkages have been studied for concretes and the recent literature proposes several models for doing so.

Three of these models have been tested in the course of the present study [2] to model the deformations measured on different formulas of reconstituted fine sandstones. The measurements were made on slender test pieces $4 \times 4 \times 70$ cm, generally on horizontal sections at the core of the different blocks, on obtained by sawing a few hours after setting, to ascertain vertical variations of the porosity relating to the vagaries of the method of preparation [3]. The formula of each sample, among which the quantity of free water, was then adjusted so as to simultaneously obtain the density of the products and their water absorptions per unit volume in 28 and 90 days, thanks to a precise water evaluation. Similarly, calculations based on the time evolution of the weight of the test pieces, allowed the assessment of the rate soaking and carbonation of the mixtures. The measurements were realized during a period exceeding two years. The test pieces were kept in open air (20 °C, 50% RH) right from the moment of their manufacture or after a 28- or 160-day curing period under water or in a watertight and an airtight package, in accordance with prescribed techniques for this type of test. The first measurement was on the shrinkage resulting from the drying of the natural rock from which was obtained the fine siliceous sands (of grain size <1 mm) used in the mixtures and then on the endogenous and drying shrinkages of the five formulas of sandstones reconstituted by associating or not white cements used in various additions, such as limestone fillers, white silica fumes, propylene polymer fibres, a superplasticizer or an antishrinkage admixture. Time evolutions of the mechanical performances of some of the formulas (tensile stress, compressive strength and modulus) were also monitored.

* Corresponding author. Tel.: +33-3-83-68-25-75; fax: +33-3-83-68-25-32.
E-mail addresses: andre.lecomte@iutnb.uhp-nancy.fr (A. Lecomte), nellyvulcano@yahoo.com (N. Vulcano-Greullet), steichen@pch.etat.lu (C. Steichen), gscharfe@vo.lu (G. Scharfe).
[1] Tel.: +352-310-502-252/200; fax: +352-317-311.

0008-8846/$ – see front matter © 2003 Elsevier Ltd. All rights reserved.
doi:10.1016/S0008-8846(03)00220-5

The first part of the article presents the materials, the mixtures, the adjustment of the formulas and the measurements carried out. The second part reconsidered the principal strength models retained, which models were initially validated on both commonly used and high performance concretes, to describe the modifications introduced to allow them to follow faithfully the dimensional variations of these particularly fine hydraulic products.

2. Materials and methods

The main characteristics of the materials selected for the fabrication of artificial sandstones are presented in Table 1. For the aggregates, two 0/1 fine sands are involved. One designated Sg, is obtained by grinding of natural sandstone that one wants reproduce. It is a partially carbonated and contains 10% fine fraction (< 80 μm). The second, denoted Sc, is often used as texture and colour corrector. It is siliceous and contains no fines. Two white cements from the same clinker were used in the mixtures: CEMI 42.5 N and CEMII/A-L 42.5 N (the designations follow the European norm EN 196-1). They respectively contain 4% and 19% limestone fillers. The specific surface of the white limestone fillers (LF) and the very pure white silica fumes (SF) incorporated into some of the formulas (SiO_2 >98%) are respectively 290 and 3400 m^2/kg. The density of the colouring pigment (P) is 4.1. The superplasticizer (SP) is a lignosulfonate and the antishrinkage (AS) is a water-free a propanediol ester polymer. Some of the stones had 1 kg/m^3 additions of short propanediol ester polymer fibres (F). Tap water was used. The granularity of the solid components is presented in Fig. 1.

The patented method [4] used for moulding the artificial stones consists in pouring a rather fluid mixture into a leak-proof mould and to remove the air from it by placing the mould in a vacuum tank submitted to appropriate vibration.

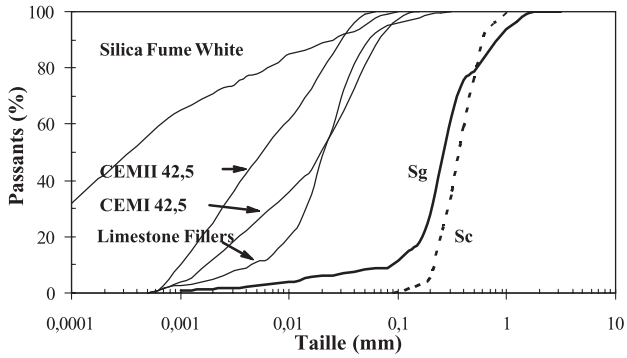

Fig. 1. The granularity of the constituents used in fabricating the artificial stones.

At the end of this treatment, the excess water is eliminated by vacuum drying with the help of a filtering carpet placed on the preparation or even a second carpet placed at the bottom of the mould. The principle is to create a depression between the membrane of the carpet and the mortar so as use the atmospheric pressure to compress the preparation to gradually liberate the intergrain residual water. The success of the method depends closely on the stability of the formula (absence of segregation) and the technology of the equipment (tightness of the mould, vibration, the vacuum drying material). These technical aspects, pushed to the limits of the system, accounted for some of the difficulties encountered during the adjustment of the method on blocks of horizontal section 60 × 100 cm. The thickness aimed at also influences the vertical homogeneity, particularly on account of the pressure exerted by the filtering carpet(s) in the packing of the grains of the skeleton as they gradually enter into contact. The packing density of the walls is generally a bit higher than that of the core of the block at least when the thickness exceeds 40 cm. These nuances are admitted for artificial stones. They however impart certain inaccuracy to the calculation of the final formula at a given death. Indeed,

Table 1
Principal characteristics of the constituents used in fabricating the artificial stones

Constituents		Sg	Sc	CEM I	CEM II	LF	SF	P	SP
Density (kg/m^3)		2550	2630	3100	3000	2700	2250	4100	1190
Absorption (%)		1.49	0.20			1.11			
Water content (%)		According to supply							144
800 μm	Passing (%)	89	96						
250 μm		46	20						
80 μm		10	0	94	100	95	100		
25 μm		6		57	85	59	90		
8 μm		4		33	57	16	82		
2.5 μm		2		15	31	6	73		
0.8 μm		0		2	5	2	63		
Specific surface (m^2/kg)		290		314	490	290	3400		
Rate (%) of limestone fillers		5	0	4	19	100			
Rate (%) of clinker				96	81				
Bogue composition	C_3S			61.8	61.8				
of the clinker	C_2S			23.4	23.4				
	C_3A			10.9	10.9				
	C_4AF			1.3	1.3				

Table 2
Formulas of the artificial stones at casting stage (dosages in m^3, masses in kg, dry aggregates)

Formulas	Constituents												Balance sheet		
	Sg	Sc	CEM I	CEM II	FC	FS	P	SP (ES)	AR	F	Free water	Air (l)	Total mass[a]	Total volume (l)	Ratio w_f/c
A	604	641	492				1.16				302	58	2049	1000	0.61
B	1071	185		489	49	15	1.08	4.04			259	60	2076	1000	0.53
C	1051	315	399				0.35			1	278	61	2049	1000	0.70
D	902	182	485				0.52		9.69		357	54	1929	1000	0.74
E	1022	207	506				0.53	1.97			297	59	2037	1000	0.59

[a] Including absorbed water.

the evaluation of the remaining water obtained by subtracting the amount of the vacuum dried water (part of which had evaporated into the vacuum pump) from the water used to make the casting and to remove the air, is only a rough estimation of the free water present in the test piece at the end of the treatment. The exact formula for each set of test pieces was the deducted from their density at 24 h and, by way of verification, from their porosity to water measured at 28 or 90 days. The steps are presented below.

3. Formulas and experiments

The dimensional variation of these fine artificial sandstones were measured on five different mixtures identified by the letters A, B, C, D, and E. The aim was to assess the influence of the mode of conservation, the packing density of the aggregate skeleton, the nature and the dosage of the cement, those of water, mineral additions, fibres and of superplasticizer admixtures or antishrinkage. These mixtures were formulated using the Compressible Packing Model (CPM) [5], involving a compaction index calibrated for each stage of the method [6]. In this way, one controls the quantity of water and admixture, when appropriate, which ensures the best mixing, casting and purging of air (compaction index of the fresh mixture). One then calculates the volume of water to vacuum dry to obtain the target packing density, which is in general close to the packing of the dry grains (compaction index after vacuum drying and air removal). For some of the formulas, the proportions of the components were chosen so as to obtain the highest packing density (which is in any case much lower than that of concretes, on account of the reduced aggregate spectrum). For others, the aim was to obtain a fresh mixture that had the best stability. A cracking index deduced from the present shrinkage measurements will also be associated with the choice of formulas [2]. Table 2 gives the dosage per cubic metre for the different constituents used in casting the five 50-cm-thick blocks, which served as test pieces. The air volumes were deduced from the density of the fresh preparations [7]. Table 3 gives the dosages after the removal of air. A standard volume of 5 l was conserved since degassing does not totally eliminate the finest bubbles the presence of which can provide some protection against frost, especially in the presence of defreezing salt [3]. Table 4 gives the quantities of water removed with the aid of the filtering carpet(s) along with the average formulas for the blocks at end of the treatment using the assessment of the remaining water.

Each of the preparations was cast into a removable, watertight metallic formwork, in six mixes of about 50 l mixed with laboratory equipment (rotary tank). Vacuum drying and the removal of air lasted a little more than an hour. At end of the treatment, the blocks, having become very firm, were then protected by curing under a few centimetres of water up to the moment of removing the formwork. This was often done 20 h from the start of the casting. The artificial stones are then firm enough for manipulation and sawing. For each of the formulas, nine samples test pieces were cut off for the shrinkage measurements from horizontal portions (slab) of the blocks, generally near the median part (Table 5). The dimension of the cross section of the test pieces was chosen to be as small as possible (4×4 cm) for the drying shrinkage to reach its maximum over a reasonable lapse of time [8] while preserving the physical integrity of the test pieces, especially at the earlier ages. The length of 70 cm facilitates an accurate

Table 3
Formulas of the artificial stones after removal of air (dosages per m^3, masses in kg, dry aggregates)

Formulas	Constituents												Balance sheet		
	Sg	Sc	CEM I	CEM II	FC	FS	P	SP (ES)	AR	F	Free water	Air (l)	Total mass[a]	V (l)	Ratio w_f/c
A	638	677	520				1.22				319	5	2166	1000	0.61
B	1133	196		518	52	16	1.14	4.27			275	5	2197	1000	0.53
C	1114	334	423				0.37			1	295	5	2171	1000	0.70
D	948	192	510				0.55		10.2		375	5	2029	1000	0.74
E	1081	218	535				0.56	2.08			314	5	2155	1000	0.59

[a] Including absorbed water.

Table 4
Vacuum-dried water and average formulas the artificial stones after removal of air (dosages per m^3, masses in kg, dry aggregates)

Formulas	Spun water	Constituents												Balance sheet		
		Sg	Sc	CEM I	CEM II	FC	FS	P	SP (ES)	AR	F	Free water	Air (l)	Total mass[a]	V (l)	Ratio w_f/c
A	76.1	693	735	565				1.33				261	5	2267	1000	0.46
B	50.5	1197	207		547	55	17	1.20	4.51			234	5	2280	1000	0.43
C	64.2	1194	358	453				0.40			1	244	5	2268	1000	0.54
D	104	1094	217	578				0.62		11.6		285	5	2203	1000	0.49
E	82.3	1218	242	593				0.62	2.30			233	5	2307	1000	0.39

[a] Including absorbed water.

measurement. After being cut, the test pieces were delicately wiped, weighed and accurately measured with a slide calliper. The length, the end and the median sections were measured. A brass slab containing a hemispherical cavity adapted to the comparator was fixed to the extremities of the pieces and their initial length L_0 measured. For each of the formulas, three test pieces were kept in status quo in open air in a room whose temperature and hygrometry were regulated at 20 ± 2 °C and 50 ± 3% RH. Depending on the series, the six remaining test pieces were either immerged in water at 20 °C or protected against drying by a double aluminium adhesive envelope, a well-tested technique for this type of test [9]. Three of these test pieces were reexposed to air in the conservation room at the age 28 days and the other three at age of 160 days. The mass of the equipment (slab and envelope) was determined by their differences in weight. The fact that the blocks were fabricated at the different dates explains certain differences in the dates of the measurements (Table 8a and b). This is particularly so for the test pieces C, D and E whose curing lasted 13, 2 and 3 days, respectively, before their preparation and submission to the tests. Table 5 gives the relevant dates adopted dictated by the mode drying the test pieces, the situation of the slabs and the type of conservation. To terminate, three test pieces (4 × 4 × 70 cm), of same natural sandstone as the sand Sg, were cut from stones newly extracted from the same quarry. They are identified by the letter N. They were kept under water at 20 °C for month before being submitted to the same conditioning and the same tests as the artificial stones.

Other types of test pieces (4 × 4 × 16 cm) were also cut out from the same slabs and kept under the same conditions. They were used in the mechanical tests, the test of frost resistance (not presented here), and for the measurements of water absorption per unit volume at 28 and 90 days realized according to the French standard B 10-503. Table 6 present these results as well as the densities of the 4 × 4 × 70 cm test pieces which were calculated from their geometry and the weight after their cutting. Formulas A and B reveal significant differences between their respective slabs. Differences exist between the other blocks as well, between the average density of the test pieces and that of the blocks (Table 4). As mentioned earlier on, these subtle differences are to be ascribed to the vagaries of the experimental method and to the imprecision in the estimation of the remaining water obtained by subtracting the vacuum dried water. They clearly show that the average formulas of the blocks do not sufficiently represent those of the test pieces submitted to the tests. A more precise calculation of the formula for each type of test piece was therefore carried out based on the density and mass balances.

Table 5
Identification of the test pieces for the dimension variation measurements

		Parameters of the codification			Designation	Sampling and measurement of L_0 at
		Vacuum drying—high = high + low	Slab, t:top, m:middle, l:low	Conservation 1 = air; 2 = water; 3 = alu; a = 28 j; b = 160 j		
Formulas	A	–	l	1	A-l1	1 day
			m	3a	A-m3a1	
			t	3b	A-t3b1	
	B	=	m	1	B = m1	1 day
			l	3a	B = l3a1	
			t	3b	B = t3b1	
	C	=	m	1	C = m1	13 days
				3a	C = m3a1	
				3b	C = m3b1	
	D	=	m	1	D = m1	3 days
				2a	D = m2a1	
	E	=	m	1	E = m1	2 days
				2a	E = m2a1	
	N			1	N1	28 days
				3a	N3a1	
				3b	N3b1	

Table 6
Density of test pieces and porosity of samples submitted to the tests

		Test pieces		Samples		
		Identification	Real density δr at 24 h (kg/m^3)	Water absorption per unit volume (NF B 10-503)		
				Age (j)/ conservation	%	$\alpha = hc \times ci(t)$
Formulas	A	-l1	2255	28/air	21.0	0.59
		-m3a1	2282	28/protection	18.6	0.66
		-t3b1	2292	28/protection	18.0	0.65
	B	=m1	2266	28/air	21.2	0.60
		=l3a1	2290	28/protection	18.3	0.65
		=t3b1	2316	28/protection	17.0	0.63
	C	=m1 =m3a1	2260	90/eau	18.9	0.82
	D	=m1 =m2a	2189	28/air	23.4	0.61
	E	=m1 =m2a	2289	28/air	18.7	0.55
	N	1 3a1 3b1	2338	–	18.0	

In this approach, we first assume that gaseous and solid constituents inside a stone are uniformly distributed, and only the quantity of water varies vertically. In other words, the relation proportions per unit volume y_i of the n solid constituents are constant everywhere in the mixture and at each stage of its elaboration. These per unit volume proportions expressed with respect to the solid volume Vs for example, are given by the relation:

$$y_i = \frac{M\mathrm{d}_i/\rho r_i}{V\mathrm{s}}, \text{ and } \sum_{i=1}^{n} y_i = 1, \text{ with } V\mathrm{s} = 1000 - a - w_{\mathrm{fa}}. \tag{1}$$

where $M\mathrm{d}_i$ represents the dry mass of the constituent i and ρr_i the real specific gravity, with a and w_{fa} representing the respective volumes of air and free water in the average formula at the relevant stage (the casting stage for instance).

3.1. Formulas of the slabs derived from the density of the fresh test pieces

Here, one relates the target quantity of the free water w_{f} of a horizontal cross section to the real fresh density δr of the test pieces extracted from the slabs. For that, it is assumed that the δr of the test pieces generally measured at 24 h (Table 6), is representative of the fresh δr. That amounts to neglecting the small quantity of curing water which may have penetrated the block following the Le Chatelier contraction occurring between the end of vacuum drying and the moment the test pieces were cut out. The δr per unit volume of slab is given by:

$$\delta r = w_{\mathrm{f}} + \sum_{i=1}^{n} \mathrm{Ms}_i(1 + \mathrm{Ab}_i) \tag{2}$$

where Ab_i is the quantity of water absorbed by the constituent i.

Combining Eqs. (1) and (2), one obtains:

$$\delta r = w_{\mathrm{f}} + V\mathrm{s}\sum_{i=1}^{n} y_i \rho r_i(1 + \mathrm{Ab}_i) \tag{3}$$

which on substitution for Vs becomes:

$$\delta r = w_{\mathrm{f}} + (1000 - a - w_{\mathrm{f}})\sum_{i=1}^{n} y_i \rho r_i(1 + \mathrm{Ab}_i) \tag{4}$$

from which one deduces:

$$w_{\mathrm{f}} = \frac{\delta r - (1000 - a)\sum_{i=1}^{n} y_i \rho r_i(1 + \mathrm{Ab}_i)}{1 - \sum_{i=1}^{n} y_i \rho r_i(1 + \mathrm{Ab}_i)} \tag{5}$$

In this way, one obtains the quantity of free water from which one derives the formula for the cross section or for any hydraulic mixture based on the fresh density (or after a 24-h curing) and the relative volume proportions of the solid and gas constituents.

3.2. Formulas of slabs derived from the porosity of hardened stones

One uses here water porosity measurements (n) realized at a given age of the on samples of hardened samples of each slab. At the fixed date, these samples, kept under the conditions recalled in Table 6, were first dried at 70 °C in order not to destabilize the hydrates, to a constant mass, then weighed and placed under vacuum during 2 h. After being immerged under vacuum, they were then kept at atmospheric pressure for 24 h. From their weight in air and in water one can calculate the porosity (French standard 10-503). It is assumed here that the variation in the volume of the sample between its setting and the moment of the test has no significant consequence on the accuracy of the test, or in other terms, that the Le Chatelier contraction occurs only in the interior of the products which maintain an apparent quasi-invariant volume. It is also assumed that in this type of product with an open porosity, almost all the vacuums are accessible to water [10], and that this water evaporates under the test conditions. These are spaces left the entrapped air (a), by water absorbed by the grains (w_{ab}), by the Le Chatelier contraction ($\mathrm{c}_{\mathrm{LCh}}$) and by the excess mixing water found in the capillaries or the small quantity adsorbed into the hydrates which we term "porosity water" (wp):

$$n = \mathrm{wp} + w_{\mathrm{ab}} + a + \mathrm{c}_{\mathrm{LCh}} \tag{6}$$

The entrapped air (a) and the water absorbed by the aggregate (w_{ab}) at the final stage of the treatment are known in the present case (Table 4). We adopt the relation proposed

Table 7
Formulas of test pieces submitted dimensional variations (dosages per m^3, masses in kg, dry aggregates)

Formulas	Slab	Constituents											Balance sheet		
		Sg	Sc	CEM I	CEM II	FC	FS	P	SP (ES)	AS	F	Free water	Air (l)	Total mass[a]	V (l)	Ratio w_f/c
A	-b	687	728	559				1.32				268	5	2255	1000	0.479
	-m	701	743	571				1.34				253	5	2290	1000	0.444
	-h	707	750	576				1.36				247	5	2292	1000	0.429
B	=m	1183	204		541	54	16	1.19	4.46			243	5	2265	1000	0.449
	=b	1207	208		551	56	17	1.21	4.55			228	5	2290	1000	0.413
	=h	1231	213		563	57	17	1.24	4.64			212	5	2317	1000	0.377
C	=m	1186	356	450				0.39			1	249	5	2260	1000	0.554
D	=m	1088	216	575				0.62		11.4		289	5	2197	1000	0.503
E	=m	1211	240	589				0.62	2.29			237	5	2299	1000	0.402

[a] Including absorbed water.

by Powers and Brownyard. [11] for estimating the Le Chatelier contraction:

$$c_{LCh} = 0.279wh \tag{7}$$

where wh is the water in the hydrates. The porosity water can be derived from the porosity measurement (n) as follows:

$$wp = n - w_{ab} - a - c_{LCh} \tag{8}$$

It remains to calculate the quantity of water mobilized by the hydrates (wh) to be able to find the free water of the fresh sample (w_f) expressed by the relation:

$$w_f = wp + wh \tag{9}$$

The quantity (wh) can be calculated from the quantity (wh_∞) which represents chemically bound water for complete hydration of the clinker to which is assigned a degree of long-term hydration (hc) which in particular depends on the ratio w/c, and a kinetic coefficient [ci(t)] which depends on the conditions of conservation of the sample and the date of the measurement:

$$wh = wh_\infty.hc.ci(t) \tag{10}$$

wh_∞ is for example given by the relation proposed by Czernin [12], reconsidered by Hua [13], starting from the composition of Bogue (in this relation, wh_∞ is expressed with respect to the quantity of hydrates):

$$wh_\infty \approx 0.24C_3S + 0.21C_2S + 0.40C_3A + 0.37C_4AF \tag{11}$$

We used the model proposed by Waller [14] to calculate the long-term degree of hydration of the clinker (h_c):

$$h_c = 1 - \exp\left(-3.38\left(\frac{w_f}{c} - \delta\right)\right) \text{ with}$$

$$\delta = \exp\left(1.63\frac{w_f}{c}\right)\frac{0.42h_{fs}fs}{c} \text{ and } h_{fs} = \min\left(1; \frac{0.23h_c}{fs/c}\right) \tag{12}$$

In the above relation, w_f and c are the dosages of the free water per unit mass and in the clinker. The quantity δ is setting coefficient taking into account the large quantity of water adsorbed by the addition, in the present case, the silica fumes (SF) while h_{fs} is the final degree of silica fumes consumption which depends on quantity of lime liberated by the clinker hydrates. The initial free water of the slab is then given by:

$$w_f = n - w_{ab} - a + (1 - 0.279)\left(\frac{wh_\infty}{1 - wh_\infty}\right) \times c\left(1 - \exp\left(-3.38\left(\frac{w_f}{c} - \delta\right)\right)\right)ci(t) \tag{13}$$

or for the Bogue composition of the white clinker used (Table 1):

$$w_f = n - w_{ab} - a + 0.235c\left(1 - \exp\left(-3.38\left(\frac{w_f}{c} - \delta\right)\right)\right) \times ci(t) \tag{14}$$

The difficulties of finding an explicit solution to this relation can for example be overcome by an iterative procedure through a step by step adjustment of the free water w_f, the quantity of the clinker c, and eventually the coefficient h_{fs} until appropriate pairs of equivalent of parameters are found. This application of this procedure gives a very satisfactory result for all the formulas (density and formulas very close to previous results) if one takes as value for kinetic coefficient ci(t), 0.73 for samples prematurely exposed to air for measurements taken at 28 days, 0.84 for those protected and measured at 28 days, 0.96 for samples kept under water and measured at 90 days. Table 6 gives the conservation modes along with the time-table for the measurements. For the test pieces measured at 28 days, these coefficients, which need to be confirmed by other tests, give plausible degrees of hydration $\alpha = hc \times ci(t)$ especially when compared to the values found in the current literature and for comparable ratios of w_f/c (see Table 6). The estimation of the hydration coefficients generally allows from the surface mass [10], the differences in weight

between the passage of the samples at 105 and 1050 °C [15], analysis of the MEB images [16], etc.

There is also a second method for adjusting the formulas of the test pieces. It is based on a simple measurement of the porosity water, especially for samples kept in open air, as is often the case with building site concretes. It is to be finally noted that these products have a high porosity, which can be explained by the low aggregate packing density and the importance of the associated residual water.

3.3. Results: the formulas of the test pieces submitted to the tests

Crossed application of the principles presented in the foregoing section has helped to refine the formulas of the test pieces submitted to the tests. The results of the calculations are presented in Table 7. Comparison with the average formulas of the blocks (Table 4) shows the interest of these verifications. It highlights certain significant differences, especially for the formulas A and B. Differences are less sharp for the formulas C, D and E, because of the improvement of the technology of the method used for the fabrication of these stones which are of a better vertical homogeneity. At the end of these adjustments, one is assured of the terms of the nine formulas on which the measurements of the dimensional variations were realized.

4. Measurements

Table 8a and b and the curves of Fig. 2a and b present the measurements of the masses and lengths measured at the various dates (the scales are logarithmic). Each value is the algebraic average of the measures on the three test pieces with a tight variance in general. After an ultimate measurement realized between 400 and around 800 days depending on the series, the test pieces were dried at 70 °C until a constant mass is reached. They were then weighed and their lengths measured and then immersed into water at 20 °C. Their weights and lengths were then measured, first at close intervals of time and then at ever increasing intervals of time. The results are not reported here. At the same time, the strength (bending tensile strength) of some of the $4 \times 4 \times 16$ cm test pieces of certain series, which were kept under identical conditions as the shrinkage test pieces, was measured at certain dates. The set of these results helped in the modelling the rises in strength and the shrinkages and also in calculating the cracking index [2]. They arouse a number of comments.

4.1. Mass of the test pieces

The weighing of the test pieces helps to know the loss of water with time, which loss can be correlated to shrinkage [17,18]. It had served in the present study to calculate the real density $\delta r(t)$ and the residual content in free water $\omega_f(t)$ expressed by its ratio to the *dry mass of the initial solid constituents* (Table 8a and b). It is a marker of the still present in the composite either in a bounded form or strongly adsorbed into the hydrates, or in free a form or weakly adsorbed into the pores. At a fixed date and for a unit volume this parameter is expressed by the following relation:

$$\omega_f(t) = \frac{w_f - (\delta r - \delta r(t))}{\delta r - w_f} \tag{15}$$

where w_f and δr are respectively the amount of free water and the real density of the formulas prior to the setting (Table 7). $\delta r(t)$ is the density measured at the date t (Table 8a and b).

4.1.1. Test pieces exposed to air from the moment of fabrication

It can be seen on the graphics of Fig. 2a that the unprotected or nonimmersed test pieces rapidly lose a great part of their water right from the moment of their fabrication, principally on account of their high porosity. This evaporation is obviously to the detriment of a satisfactory hydration of the clinker. One can seek to evaluate the rate of hydration α_{h1} reached at the "point of equilibrium" which appears when density stabilizes (Fig. 3) from the density of the test pieces. As initial hypothesis, we consider this point as marking the end of the exchange of water with the surrounding medium. The remaining porosity water (wp) is then roughly the quantity extracted by completely drying the test pieces at 70 °C to a constant weight at the date n. Certainly, as will be seen further on, shrinkage due to drying and the mechanical strengths continue to evolve beyond the equilibrium point. But the amount of water consumed is very low compared to the amount consumed and evaporated before the equilibrium point [19]. The corresponding water content ω_{wp} is then calculated simply as the difference between residual free water contents before the drying $\omega_{wf}(n-1)$ and after the drying $\omega_{wf}(n)$:

$$\omega_{wp} = \omega_{wf}(n-1) - \omega_{wf}(n) \tag{16}$$

By subtracting the porosity water content from the lowest residual free water content recorded during the test (equilibrium point), one obtains a good approximation of the water content of the hydrates (Fig. 3):

$$\omega_{wh} = \min_{i=1}^{n-1} (\omega_{wf} i) - \omega_{wp} \tag{17}$$

The mass of water in the hydrates in a unit volume of stone is obtained by multiplying ω_{wh} by the density of solid constituents, that is:

$$\mathrm{wh} = \omega_{wh}(\delta r - w_f) \tag{18}$$

Table 8a
Table of measurements realized on formulas A, B and C

Conservation in air						Protection during 28 days followed by exposure to air						Protection during 160 days followed by exposure to air					
Age d	δr kg/m^3	ω_f %	$\Delta L/L$ 10^{-6}	ft MPa	fc MPa	Age d	δr kg/m^3	ω_f %	$\Delta L/L$ 10^{-6}	ft MPa	fc MPa	Age d	δr kg/m^3	ω_f %	$\Delta L/L$ 10^{-6}	ft MPa	fc MPa
A = l1						*A = m3a1*						*A = t3b1*					
1	2255	13.5				1	2282	12.5				1	2309	11.1			
1.2	2238	12.7	0	2.4	14.0	1.2	2281	12.5	0			1.2	2299	10.6	0	3.0	19.0
3	2131	7.29	− 236	2.5	31.9	3	2281	12.5	− 14			3	2299	10.6	− 18	5.0	47.5
7	2113	6.40	− 447	2.8	39.6	7	2281	12.5	− 23			7	2299	10.6	− 26	5.0	56.3
14	2103	5.89	− 646	3.6	36.8	14	2281	12.5	− 21			14	2299	10.6	− 28	5.7	60.5
28	2099	5.67	− 764	3.9	39.9	28	2281	12.5	+ 9	5.0	62.4	28	2299	10.6	− 5	6.0	67.7
30	2099	5.66	− 782	3.2	36.7	30	2253	11.2	− 205	4.8	64.9	59	2299	10.6	+ 2	5.0	63.9
36	2099	5.69	− 808	3.7	38.4	36	2234	10.2	− 419	4.8	65.1	90	2299	10.6	+ 18	5.7	75.1
59	2101	5.75	− 843	3.5	42.3	59	2213	9.16	− 690	5.0	67.3	160	2299	10.6	− 6	5.5	78.2
90	2104	5.90	− 888	4.1	44.8	90	2204	8.75	− 794	5.5	80.6	161	2298	10.6	− 191		
160	2111	6.26	− 952	4.2	54.3	160	2197	8.41	− 870	6.0	81.1	163	2292	10.3	− 294		
299	2123	6.89	− 988	5.8	65.9	299	2196	8.32	− 872	6.1	82.7	167	2284	9.92	− 409		
450	2133	7.39	− 1077			450	2194	8.25	− 925			188	2267	9.10	− 604		
805	2146	8.04	− 1240			600	2190	8.02				226	2262	8.84	− 670	5.8	74.6
809	2125	6.96	− 1628			938	2186	7.84				400	2245	8.04	− 780		
						948	2157	6.41				806	2240	7.80	− 815		
												889	2208	6.26	− 966		
B = ml						*B = l3a1*						*B = t3b1*					
1	2266	12.2				1	2290	9.95				1	2316	9.60			
1.2	2252	11.5	0	1.8	10.3	1.2	2289	9.90	0			1.2	2306	9.12	0	3.1	23.6
2	2147	6.32	− 243	2.4	23.6	2	2288	9.88	− 43			2	2306	9.12	− 31	4.1	40.1
5	2126	5.40	− 503			5	2289	9.90	− 43			5	2307	9.16	− 31		
7	2115	5.17	− 682	3.2	33.7	7	2288	9.88	− 40			7	2306	9.15	− 21	4.2	57.0
14	2105	4.65	− 999	4.8	44.0	14	2288	9.88	− 43			14	2306	9.15	− 26	4.7	70.2
28	2102	4.51	− 1004	4.4	45.5	28	2288	9.88	− 25	5.0	63.2	28	2306	9.13	− 16	4.9	69.8
30	2102	4.51	− 1023	5.1	41.8	30	2264	8.82	− 332	4.6	65.6	58	2306	9.13	− 1	5.7	82.8
36	2102	4.53	− 1029	4.2	39.7	36	2246	8.04	− 534	5.0	67.2	90	2306	9.13	+ 3	5.9	76.3
58	2105	4.65	− 1089	5.1	52.1	58	2226	7.16	− 789	5.4	71.6	159	2306	9.13	− 12	6.0	85.6
90	2109	4.86	− 1091	4.7	45.2	90	2217	6.76	− 910	5.5	79.9	160	2306	9.13	− 185		
153	2118	5.29	− 1146	4.6	46.5	153	2210	6.46	− 994	5.5	82.1	162	2299	8.79	− 304		
299	2131	5.95	− 1184	4.3	61.4	299	2207	6.34	− 1006	5.6	87.5	166	2290	8.39	− 428		
450	2142	6.47	− 1258			450	2206	6.30	− 1046			187	2270	7.44	− 646		
804	2154	6.70	− 1414			600	2204	6.20	− 1070			225	2262	7.06	− 743		
808	2135	5.74	− 1854			938	2199	5.98	− 1080			299				6.1	83.2
						948	2169	4.66	− 1260			400	2225	6.23	− 847		
												806	2231	6.01	− 861		
												889	2206	4.40	− 1079		
C = m1						*C = m3a1*						*C = m3b1*					
1	2265	12.5	0			1	2275	12.3	0			1	2264	12.7	0		
13	2265	13.1	0	4.6	40.0	13	2275	12.3	0			13	2260	12.7	0		
15	2227	11.3	− 149			15	2271	12.1	− 30			15	2260	12.7	− 18		
20	2198	9.82	− 330			20	2271	12.1	− 32			20	2260	12.7	− 26		
28	2175	8.68	− 482			28	2271	12.1	− 14			28	2260	12.7	− 3		
41	2161	7.98	− 623	4.91	51.0	41	2271	12.1	− 31	5.1	44.7	41	2260	12.7	− 11	4.9	45.0
43	2160	7.93	− 653			43	2243	10.7	− 128			43	2260	12.7	− 24		
50	2157	7.76	− 675			50	2211	9.17	− 297			50	2260	12.7	− 10		
73	2152	7.49	− 756	5.0	58.9	73	2181	7.65	− 603	5.4	47.1	73	2260	12.7	− 25	5.2	46.0
103	2150	7.40	− 797			103	2171	7.18	− 712			103	2259	12.7	− 10		
172	2146	7.23	− 852	5.0	58.2	172	2164	6.82	− 795	5.3	52.2	172	2258	12.61	− 27	5.5	50.0
300	2132	6.52	− 872			400	2155	6.38	− 850			300	2150	7.241	− 750		
621	2149	7.35	− 915			718	2148	6.03	− 929			450	2142	6.84	− 802		
706	2119	5.87	− 1184			728	2127	5.19	− 1143			619	2137	6.59	− 829		
												623	2107	5.11	− 1069		

Table 8b
Table of measurements realized on formulas D, E and N

Conservation in air							In water for 28 days during followed by exposure to air				In water for 160 days followed by exposure to air						
Age d	δr kg/m^3	ω_{eff} %	$\Delta L/L$ 10^{-6}	ft MPa	fc MPa	E GPa	Age d	δr kg/m^3	ω_{eff} %	$\Delta L/L$ 10^{-6}	Age d	δr kg/m^3	ω_{eff} %	$\Delta L/L$ 10^{-6}	ft MPa	fc MPa	E GPa
D = m1											*D = m2b1*						
3	2198	12.9	0								3	2183	13.1	0			
6	2059	7.64	− 174	2.8	30.9	17.3					6	2194	14.7	+147	3.2	28.1	20.3
14	2038	6.61	− 400								14	2202	15.1	+183			
28	2026	6.09	− 585	3.9	41.6	21.6					28	2203	15.2	+304	4.5	42.5	25.1
90	2027	6.04	− 727	4.0	39.2	21.8					90	2209	15.5	+378	4.7	50.6	26.9
118	2029	6.13	− 767								160	2212	15.7	+395			
385	2045	7.00	− 997								350	2062	8.75	− 454			
389	2020	5.76	− 1438								450	2072	8.44	− 524			
											455	2037	6.52	− 614			
E = m1											*E = m2b1*						
2	2297	11.2	0								2	2281	10.4	0			
6	2186	7.19	− 335	3.5	45.6	24.9					6	2286	12.2	+149	4.1	46.8	27.4
14	2171	6.46	− 600								14	2291	12.5	+181			
28	2163	6.05	− 786	4.8	55.5	27.9					28	2292	12.5	+239	5.5	60.4	29.9
90	2161	5.96	− 925	4.8	60.3	29.0					90	2297	12.8	+338	5.4	66.4	31.8
118	2162	6.03	− 963								160	2301	12.9	+367			
385	2169	6.62	− 1154								350	2175	7.75	− 586			
389	2133	4.88	− 1464								450	2182	7.41	− 650			
											455	2159	5.96	− 808			
N1							*N3a1*				*N3b1*						
1	2345	5.7	0				1	2337	5.7	0	1	2332	7.39	0			
1.2	2231	0.6	− 31				1.2	2337	5.1	− 22	1.2	2332	7.39	− 22			
4	2218	0	− 74				4	2336	5.1	− 30	4	2331	7.36	− 31			
8	2218	0	− 126				8	2337	5.1	− 27	8	2331	7.38	− 28			
15	2218	0	− 127				15	2337	5.1	− 22	15	2331	7.38	− 25			
29	2218	0	− 135				29	2336	5.1	− 23	29	2331	7.38	− 24			
38	2218	0	− 140				38	2175	0	− 207	57	2331	7.38	− 15			
57	2218	0	− 140				57	2175	0	− 196	160	2231	7.36	− 24			
160	2218	0	− 139				92	2175	0	− 199	180	2172	0	− 173			
							830	2177	0	− 191	834	2171	0	− 151			
							834	2176	0	− 164							

The rate of hydration α_{h1} at the equilibrium point can then be written as:

$$\alpha_{h1} = \frac{wh/(c+wh)}{wh_{\infty}} \tag{19}$$

wh_{∞} is defined by Eq. (11). It can moreover be observed that beyond the equilibrium point, generally about 40 days, the test pieces progressively increase in weight. Conditions of conservation being regular (20 °C, 50% RH), this can only be due to carbonation with hydrated phases of the air. Coloration test with alcoholic solution of phenolphthalein on freshly sawn sections of the $4 \times 4 \times 16$ cm test pieces kept for 160 days in air did confirm a fairly well spread and noticeable diminishing of pH (attributing to $Ca(OH)_2$ consumption), by comparison to sections of test pieces protected for 160 days. Exploiting further the weights, one may wish to find an *indicative* rate of carbonation reached at the end of the tests by computing the ratio of the quantity of carbonated Portlandite $(Ca(OH)_2)_{carb}$ to the total quantity of Portlandite formed $(Ca(OH)_2)_{tot}$. We assume that CSH and aluminates react much less to carbonation than Portlandite [20]. This coefficient is equal to:

$$\alpha_{carb} = \frac{(Ca(OH)_2)_{carb}}{(Ca(OH)_2)_{tot}} \tag{20}$$

Let us recall the carbonation reaction:

$$Ca(OH)_2 + CO_2 \rightarrow CaCO_3 + H_2O$$

or, after dissolving: (21)

$$Ca^{2+} + CO_3^{2-} + H_2O \rightarrow CaCO_3 + H_2O$$

the molar weights of different constituents being 74, 44, 100 and 18, respectively for Portlandite, carbon dioxide, calcium carbonate and water. We consider that major part of the water liberated by this reaction remains in the medium and hydrates an extra amount of the binder. The observed

increase in weight in this case roughly results from the entry of a certain mass of carbon dioxide (M_{CO_2}), into the system. But must logically also deduct a certain of water taken out of the system. The latter is unknown. (M_{CO_2}) is therefore under-estimated.

The minimal CO_2 content fixed by the Portlandite, ω_{CO_2}, expressed in terms of the mass of dry solid constituents (Fig. 3), is in this case the difference between the final content in residual free water before drying and the equilibrium point content in residual free water.

$$\omega_{CO_2} \geq \omega_f(n-1) - \min_{i=1}^{n-1}(\omega_f i) \tag{22}$$

The corresponding mass of CO_2 per unit volume (M_{CO_2}), is obtained by multiplying ω_{CO_2} by the density of the solid constituents, as in:

$$M_{CO_2} = \omega_{CO_2}(\delta r - w_f) \tag{23}$$

δr and w_f are as previously defined.

Finally, by considering the relation of proportionality between the molar weights of $Ca(OH)_2$ and CO_2, and also H_2O and CO_2, one obtains the minimal weight of Portlandite transformed into carbonate $(Ca(OH)_2)_{carb}$ and the weight of water liberated by the carbonation reaction (w_{carb}):

$$(Ca(OH)_2)_{carb} = \frac{74}{44} M_{CO_2} \approx 1.68 M_{CO_2} \text{ and}$$

$$w_{carb} = \frac{18}{44} M_{CO_2} \approx 0.41 M_{CO_2} \tag{24}$$

The long-term rate of hydration α_{h2} can then be written as:

$$\alpha_{h2} = \frac{(wh + w_{carb})/(c + wh + w_{carb})}{wh_\infty} \tag{25}$$

The amount of Portlandite supplied by a hydrated clinker is generally estimated to be roughly 25% of the quantity of hydrates [20]. In the present case, that comes to $1.235.c$ (according to Eq. (14)). Taking α_{h2} as the hydration rate gives:

$$(Ca(OH)_2)_{tot} \approx 0.25.1.235.c.\alpha_{h2} \approx 0.31.c.\alpha_{h2} \tag{26}$$

where c is the weight of the clinker.

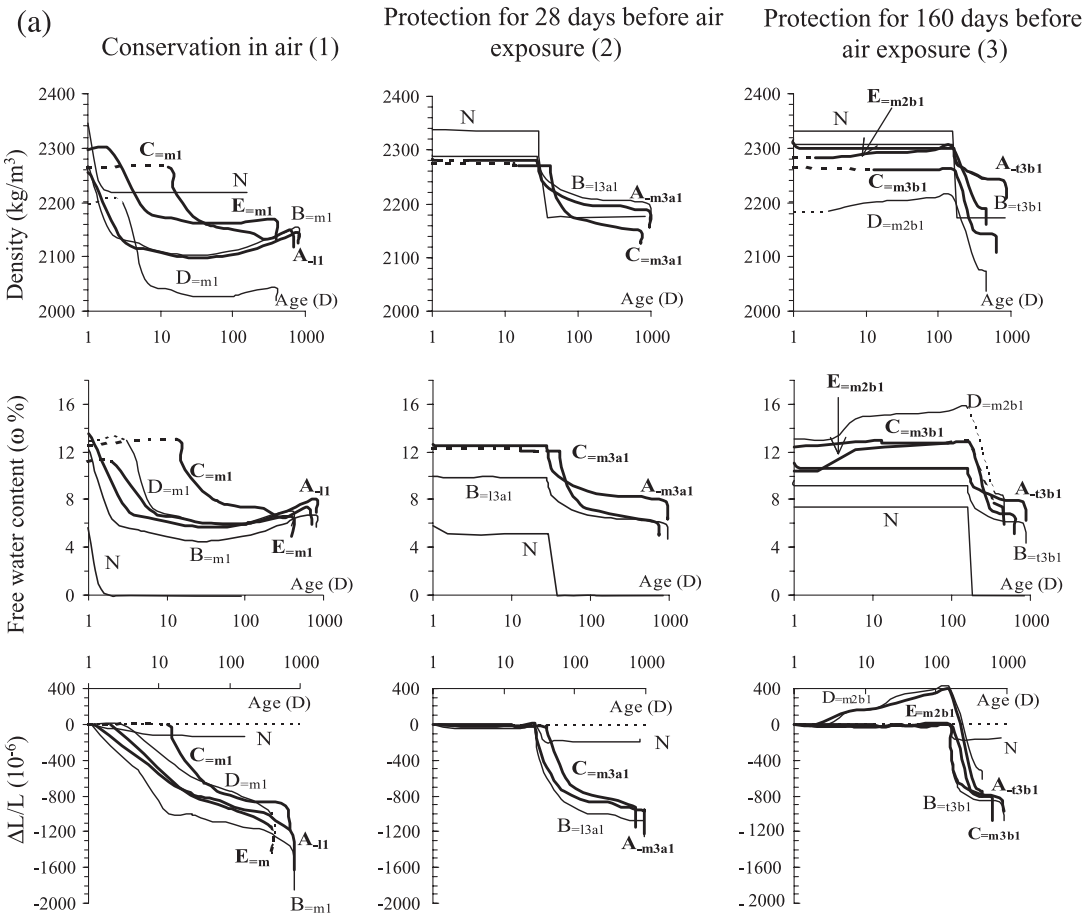

Fig. 2. (a) Evolution of the characteristics of the mixtures as function mode of conservation. (b) Evolution of the characteristics of the mixtures as function mode of conservation.

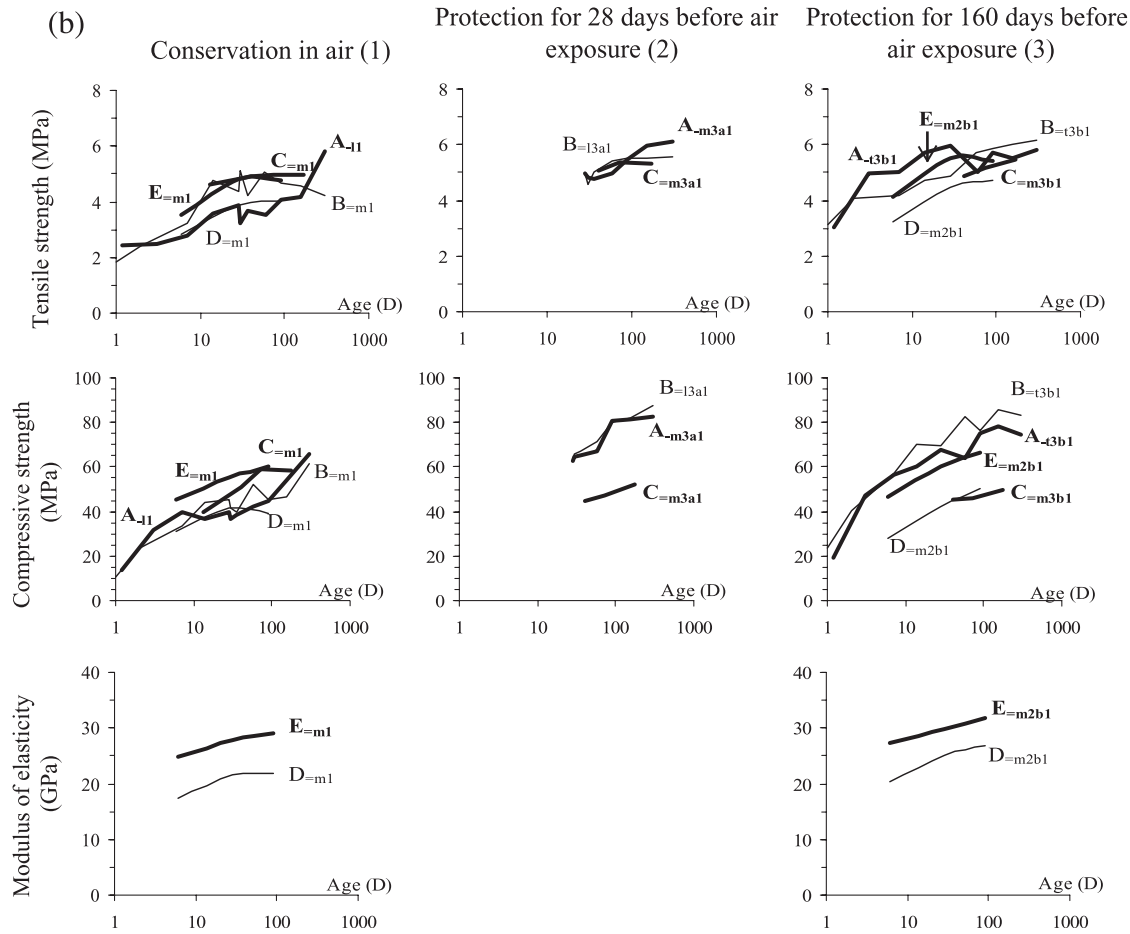

Fig. 2 (*continued*).

The rate of carbonation α_{carb} is then derived from weights through the relation:

$$\alpha_{carb} \geq \frac{1.68\left(\omega_f(n-1) - \min_{i=1}^{n-1}(\omega_f i)\right)}{0.31.c.\alpha_{h2}} \quad (27)$$

Certainly, the present approach is global and simplifying. It can only give an average indication about the rates of hydration and carbonation. We in fact assumed that the hydration of the Portlandite and of the CSH follows the same kinetics when the water content diminishes, and that the major part of the water liberated by the carbonation reaction remains in the system. Moreover, we also know that the phenomena of evaporation and carbonation are not homogeneous in all parts of a composite material, and much less between the core of the pieces and their periphery. But in the case of these tests pieces which are of small radius and made up of a mixture of fine and porous grains, their water and carbonation profiles can be thought of as being rather regular, when compared to those of more compact materials of higher radius. The rates of hydration obtained and the corresponding porosities, as presented in Table 9, are quite in agreement with those derived from water porosity measurements (Table 6) realized at dates close to the equilibrium point. These porosities per unit volume (n), are calculated using the relation:

$$n \approx w_f - \Delta V_{h1} + a + w_{ab} = \text{eff} - 0.235.c.\alpha_{h1} + a + w_{ab} \quad (28)$$

where w_f, ΔV_{h1}, a and w_{ab} are respectively the volume free water before the setting, the increase in the solid volume of the clinker due to hydration, the volume of residual air and

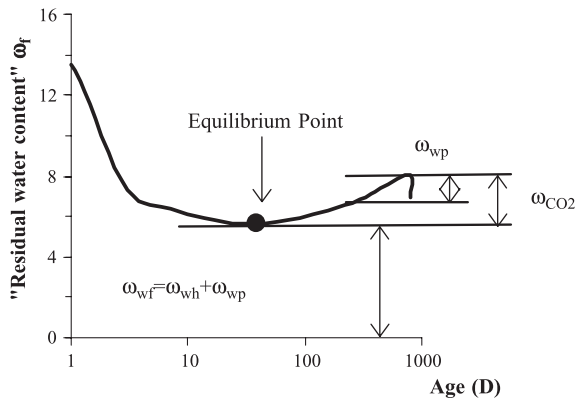

Fig. 3. Evaluation of Portlandite fixed water and CO_2 contents, expressed as a ratio of dry solid constituents, calculated from the weights of test pieces exposed to air right from their fabrication.

the volume of water absorbed by the aggregates. Finally, with the same reasoning, one can also derive, from the measurements, the packing density ϕ (excluding the internal porosity). For that, subtract from the unit volume, the volume of free water and of occluded air and add the increase in volume due to the final hydration of the cement ΔV_{h2} and that due to the carbonation of the Portlandite ΔV_{carb}. The latter term is found by considering the molar volumes of the calcite and the Portlandite and their respective densities, which are 2.715 and 2.23. Table 9 gives the corresponding results. On can then write:

$$\phi \approx 1000 - w_f - a + \Delta V_{h2} + \Delta V_{carb} \text{ with } \Delta V_{carb} = \frac{Ca(OH)_2}{2.23}\alpha_{carb}\frac{100/2.715}{74/2.23} = \frac{1.68M_{CO_2}\times 100}{2.715\times 74} = 0.836.M_{CO_2} \quad (29)$$

This thus validates the coherence of the processing of the weights recorded. These data provide a backing for certain descriptions. They also show that, in the absence of the means for conducting more sophisticated investigations, simple weights of the test pieces and measurements of their porosity to water, recorded at appropriate the time intervals and dates between the setting and the long term, can indeed provide interesting and likely quantitative parameters.

4.1.2. Test pieces exposed to air for 28 or 160 days

These test pieces also undergo a rapid loss in weight right from their exposure to air (Fig. 2a), but contrary to the preceding test pieces, the weight stabilizes after a few months of drying with the appearance of no clear critical point. They have therefore not undergone any significant carbonation a priori. The development and the consolidation of the CSH in the presence of a sufficient quantity of water seem to limit this reaction. The porosity and the permeability of the stone to air are therefore reduced, thereby delaying the carbonation or limiting it to the periphery of the test pieces. One can however determine the hydration rate α_{h2}, the porosity and the packing density at the long term by applying the preceding relations. The corresponding values are given in Table 9.

4.1.3. Results

Concretely, one observes for the artificial sandstones which were not protected right from their fabrication, a relatively low hydration rate α_{h1} at the critical point, with α_{h1} situated between 0.56 and 0.62 according to the w/c ratio (Table 9). The mixture C, which was kept in cure for 13 days, presents a shifted critical point with a hydration rate of 0.80, the corresponding porosity being 19.1. That of the other formulas is situated between 18.6 and 23.4. At the end of the drying, the carbonation rate α_{carb} seems to be directly related to the duration of the curing and the cement dosage; it is 0.7 for 1-day exposed test pieces, and about 0.3 for (the cement rich) 2- or 3-day exposed test pieces or (the cement poor) 13-day exposed pieces. Carbonation significantly improves the final hydration rates α_{h2}, by lowering the porosity from 0.4 to 1.3 points and increasing the solid volume so that the final densities are close to those of the test pieces cured during 28 or 160 days.

For these mixtures (cured 28 or 160 days), the loss of weight on exposure to air is sharply less important. The "hydration water content ω_{wh}" is therefore higher, which proves that the binding phase is of a better hydration. The coefficients α_{h2} are between 0.72 and 0.82, and the packing densities between 0.828 and 0.859 according to the w/c ratios. Differences between a 28- and 160-day curing are slight.

Finally, there exist differences between the formulas of the unprotected test pieces in particular. Thus, formula A globally presents the same density over time as B even though the latter contained less water at the beginning and a lower free residual water over time In fact, the presence of additions (LF, SF) did not increase the packing density of this stone as expected, because the proportions of the two sands which initially led to the maximal packing density of the aggregate mixture were modified to assure the stability

Table 9
Formulas, « free water and CO_2 contents », rates of hydration and carbonation, porosities and final packing density derived from the weights of the test pieces

Formulas					ω_{ep}	ω_{wh}	Critical point			Terms relating to drying					
Reference	c kg/m^3	w_f kg/m^3	w_f/c	Cure (day)			Age	α_{h1}	n %	Age	ω_{CO_2}	α_{h2}	α_{carb}	n %	ϕ
A=l1	559	268	0.479	1	1.1	4.6	30	0.62	20.7	800	2.4	0.73	0.68	19.4	0.858
A=m3a1	571	253	0.444	28	1.4	6.4	–	–	–	950	–	0.82	–	16.6	0.846
A=t3b1	576	247	0.429	160	1.5	6.3	–	–	–	800	–	0.81	–	15.9	0.853
B=m1	541	243	0.449	1	1.0	3.6	30	0.61	21.2	800	2.2	0.73	0.78	19.9	0.856
B=l3a1	551	228	0.413	28	1.3	4.7	–	–	–	950	–	0.75	–	17.2	0.846
B=t3b1	563	212	0.377	160	1.6	4.4	–	–	–	800	–	0.72	–	15.9	0.859
C=m1	450	249	0.554	13	1.5	5.0	200	0.80	19.1	700	0.8	0.85	0.25	18.7	0.846
C=m3a1				41	1.0	5.0	–	–	–	720	–	0.81	–	18.4	0.828
C=m3b1				172	1.5	5.1	–	–	–	600	–	0.82	–	18.3	0.833
D=m1	575	289	0.503	3	1.2	4.8	90	0.60	23.4	400	1.0	0.65	0.29	22.9	0.803
D=m2a				160	1.9	6.5	–	–	–	450	–	0.79	–	21.1	0.806
E=m1	589	237	0.402	2	1.7	4.2	90	0.56	18.6	400	0.7	0.59	0.25	18.2	0.848
E=m2a				160	1.4	6.0	–	–	–	450	–	0.75	–	16.1	0.858

of the mortar for the casting stage [3]. The formula D has the lowest density, since at the end of the treatment, it contained the highest amount of water. But this water does not evaporate in the same proportions as the other mixtures, without doubt, on account of the presence of antishrinkage admixture, which is known to modify the surface tension of water.

These results show the necessity to keep the artificial stones in cure for two to three weeks for the binding phase to reach a satisfactory hydration, the porosity minimized and to limit the carbonation. When the carbonation is important (test pieces prematurely exposed to air), it shows on the surface in the form of cullet which generates efflorescences and unsightly rings for a quality product.

Moreover, it is to be noted that natural sandstone dries up completely in a few hours provided it is in contact with air. Its high and open porosity, which is corroborated by capillarity and mercury porosity tests [3], explains this result.

4.2. Dimensional variations

The corresponding tests show in the first place that natural sandstone presents a nonnegligible drying shrinkage of the order of 150 to 200 10^6. It gets stabilized only after one week drying, no matter the conditions of prior conservation. Sand obtained from this sandstone for reconstituting the stone contains free grains of silica and calcite, comprising grains of size less than or equal to 400 μm and grains of size bigger than 400 μm [21] in a proportion of 70/30. The measured shrinkage of natural sandstone test pieces must therefore be taken into account in the total shrinkage of artificial stones (in proportion to the volume of the latter present in the mixtures, in the absence of another approach). Artificial sandstones prepared with hydraulic binders have much higher total shrinkage than natural stones and vary in amplitude in function of the formula and the mode of conservation.

For the unprotected test pieces, their long-term maximum, before being dried in the drying room, is between 1000 and 1400×10^{-6}. After their drying, the shrinkage for formula B reaches more than 1800×10^{-6}. The shrinkage kinetic varies depending on the formula, with the extreme case of formula B which contains additions and for which the shrinkage is the most precocious and the most pronounced. The formula D, which contains an antishrinkage admixture, has a delayed shrinkage but in the long run the amplitude is comparable to that of the other stones. Formula C, which incorporates fibres, presents the smallest final shrinkage (820×10^{-6}). We recall that its drying began only after 13 days of curing. Al the same it is the formula that still presents the smallest final shrinkage, even after complete desiccation. Moreover, its visible and very short fibres (<1 mm, can be burned on the surface, if need be), assures a homogeneous shrinkage, so that non-micro-crack whatsoever can be seen on the huge stones exploited on construction fields in contrast to other formulas, for which the beginning of cracks at regular intervals can sometimes be detected, particularly at moments of pronounced hydric changes. Fibres thus constitute an interesting solution for attenuating the shrinkage effect of these products.

We recall that these are just relative comparisons between raw measurements realized on these stones. Only a realistic modelling of the dimensional variations that integrates the different terms of the formula can allow understanding of the role of each of the components and, in the end, help identify those mixtures that less prone to shrinkage.

For test pieces of small section, it can be taken that, under the conditions of laboratory conservation, the quasi-totality of desiccation shrinkage of these pieces is reached after 450 days of drying. Indeed, referring to the kinetic functions of the models of total shrinkage, like that of CEB-FIB [22] recalled below, for a section of 4×4 cm^2, one obtains at the same date (after 450 days of drying), 98.5% of the total shrinkage:

$$\beta_{ds}(t - t_s) = \left(\frac{(t - t_s)/t_1}{350(h/h_0)^2 + (t - t_s)/t_1} \right)^{0.5} \quad (30)$$

with $h_0 = 100$ mm and $h = 2A_c/u$. A_c and u, respectively denote the cross-section area (mm^2) and the perimeter (mm) of the test pieces in contact with external medium. $(t - t_s)$ is the duration of the drying with $t_1 = 1$.

However, for the test pieces which were not protected since their fabrication, it was observed that the total shrinkage did not stabilize at this date, but continued to evolve significantly to the last measurements near 800 days, which contradicts the preceding calculation.

Could it be the loss of part of the water liberated by the carbonation that provoked the additional shrinkage while the solid volume and the strength (see further below) continued to increase?

The test pieces protected for 28 or 160 days showed very small dimensional variations up to the moment of their exposure to air (Table 8a and b and Fig. 2). Despite their small ratios w/c, they thus underwent little endogeneous shrinkage, except if this had happened between the setting and the moment the initial lengths were measured at 24 h (formulas A and B). It is indeed known that, in massive pieces, such shrinkage can develop, in a short term, in a substantial manner, on account of heat activation. However, the long-term shrinkage of these test pieces is less than that of those prematurely exposed to air, probably because they have a better mechanical strength. The differences described between the preceding formulas are found again with the present formulas too. Once again, the advantage is on the side of stones with fibre fillers.

The test pieces conserved in water (formulas D and E) swell up to 400×10^{-6} in 90 days. The total dimensional variation exceeds 1500×10^{-6}.

It is finally noteworthy that at end of the tests, despite the important shrinkages, none of the test pieces presented any rupture, nor apparent cracks. The small section of the test

pieces, the four faces of which are exposed to the ambient surrounding, and their high porosity favoured the homogeneity of the development of the desiccation and the associated shrinkage.

On the contrary, such disorders sometimes appear on stones used in constructions. Their big size can lead to a cracking of the skin (differential shrinkage) of unprotected faces after a dry period. In addition, they are often fixed on more rigid concrete supports. This can create a stifled shrinkage going as far as ruining the product if it is submitted to an additional external mechanical stress.

4.3. Mechanical performances

In general, as can be expected, the mechanical performances of stones kept in open air right from their fabrication are lower than those of stones protected or kept in water for 28 or 160 days. For example, for the formula B which contains some additions, if it is not exposed to air after its fabrication, its compressive strength at 28 days is 75 MPa and the long-term strength close to 100 MPa. If on the contrary, it is exposed to air after its fabrication, compressive strength at 28 days is only 40 MPa and increasing to attain 60 MPa at 300 days. This behaviour may be related to the phenomenon of carbonation which reduces the porosity and thereby increases the strength. The water liberated but not evaporated may also form new CSH with the clinker and/or allow the continuation of the pouzzolanic reaction with the additions present. The overall evolution of the tensile strength follows that of the compressive strength with the exception of the fibred formula C which shows an interesting gain. Notice that the bending tensile strength measurements realized on the $4 \times 4 \times 16$ prisms were weighted by a scale effect coefficient of 0.58 which gives, to a good accuracy, the values normally obtained by cleaving on cylinders, 16 cm in diameter and 32 cm in height [23].

The elastic modulus measured on formulas D and E increases also with the compressive performance, with the test pieces conserved in water showing a higher performance than those kept in air after their fabrication.

5. Conclusion

The aim of the calculations was to establish the exact terms of the formula for each set of test pieces submitted to the tests of dimensional variations. We determined the postsetting density and the posthardening porosity to water, that is, two simple tests which allow the determination of the free water of the mixtures. Parallel observation of the time evolution of the weights of the test pieces often shows, especially for test pieces exposed to air at an early age, the existence of a point hydric equilibrium. By calculating the residual water content at this instant (the equilibrium point) and after a moderate temperature complete desiccation realized later, one can derive a reasonable degree of hydration. The calculations are based on commonly admitted hypotheses concerning the hydration of hydraulic binders. Similarly, an estimation of the volume of hydrates, as a function of the degree of hydration, helps to determine the porosity which turns out to be close to that measured at dates near the critical point. Finally, the increase in the volume of the test pieces beyond the critical point allows the estimation of a degree of carbonation and the final packing density of the stones. The proposed methodology constitutes a coherent set based on simply weighing the test pieces and measuring associated shrinkages.

The shrinkage measurements showed that these formulas presented no or little apparent endogenous shrinkage. The desiccation shrinkage, which starts immediately with exposure to air, is on the contrary very high. The final amplitude depends on the time interval between the fabrication and the exposure to air. Globally, the long-term shrinkages for the same duration of exposure to air are comparable for all the formulas excepting formulas with fibre additions for which the final amplitude is significantly less pronounced.

Finally, the mechanical strengths depend none only on the composition, but also on the mode of conservation.

These data have allowed the adjusting of the different models used in order to reproduce more faithfully observed evolutions [2]. The helped determine a cracking index and to study the respective roles of each of the constituents.

References

[1] A.M. Neville, Properties of Concrete, Longman, Harlow, UK, 1995.
[2] A. Lecomte, N. Vulcano, C. Steichen, G. Scharfe, The risk of cracking of fine hydraulic mixtures, Cem. Concr. Res. 33 (2003) 1982–1996.
[3] N. Vulcano-Greullet, Elaboration d'un procédé de fabrication de pierres reconstituées à base de liant hydraulique, application au grès d'Ernzen, thesis of the University Henri Poincaré Nancy, 2001.
[4] A. Lecomte, N. Vulcano, G. Feidt, G. Scharfe, C. Steichen, M. Pirotte, Method for Producing Artificial Stones, 2000, WO 00/050356.
[5] F. de Larrard, Concrete mixture proportioning, a scientific approach, Modern Concrete Technology, vol. 9, E & FN Spon, London, 1999.
[6] A. Lecomte, N. Vulcano, Compactabilité de mélanges granulaires fins, Sym. Phys. Méca. Mat. Gran, ENPC Paris (2000) 327–332.
[7] A. Lecomte, Ajustement des méthodes de formulation de béton au m^3 en tenant compte du volume réel, Ann. BTP 5 (1998) 13–26.
[8] R. Le Roy, Déformations instantanées et différées des bétons à hautes performances, ER LPC OA 29 (1996).
[9] F. Toutlemonde, F. Le Mahou, Protection des éprouvettes vis-à-vis de la dessiccation, BLPC 203 (1996) 105–119.
[10] V. Baroghel-Bouny, A. Ammouche, H. Hornain, J. Gawsewitch, Vieillissement des bétons en milieu naturel: une expérimentation pour le XXIème siècle, BLPC 228 (2000) 71–86.
[11] T.C. Powers, T.L. Brownyard, Studies of the physical properties of hardened Portland cement paste, Proc. ACI 41 (1946).
[12] W. Czernin, Cementkemi för byggare, Svenska Cementföreningen, 1959.
[13] C. Hua, Analyse et modélisation du retrait d'autodessiccation de la pâte de ciment durcissante, ER LPC OA 15 (1995).
[14] V. Waller, Relation entre composition, exothermie en cours de prise et résistance à la compression des bétons, thesis of the Ecole Nationale des Ponts et Chaussées, Paris, 1999.

[15] C. Hua, P. Acker, A. Ehrlacher, Retrait d'autodessiccation du ciment, BLPC 196 (1995) 79–90.
[16] A. Ammrouche, N. Rafai, H. Hornain, T. Chaussadent, G. Platret, V. Baroghel-Bouny, Comparaison de différentes méthodes de mesure du degré d'hydratation de pâte de ciment Portland durcies, Rev. Fran. Génie. Civil. 5 (2002) 205–216.
[17] M. Buil, Contribution à l'étude du retrait de la pâte de ciment durcissante, RR 92, LCPC, Paris, 1979.
[18] L. Granger, Comportement différé du béton dans les enceintes de centrales nucléaires: analyse et modélisation, thesis of the Ecole nationale des Ponts et Chaussées, Paris, 1995.
[19] G.L. Verbeck, R.H. Helmuth, Structure and physical properties of cement paste, Fifth Inter Sym Chem Cement, Session III.1, Tokyo, 1968.
[20] V. Baroghel-Bouny, Caractérisation des pâtes de ciment et de bétons, LCPC Press, Paris, 1994.
[21] A. Lecomte, J.M. Mechling, Analysis of the granular structures of aggregates using solid volume measurement of elementary fractions, CCA, ASTM 23 (2) (2001) 105–112.
[22] CEB-FIP Model Code 1990, CEB Bull. Inf. 213/214, Switzerland, 1993.
[23] A. Lecomte, Valorisation des ressources minérales de la Lorraine et du Luxembourg, Habilitation à diriger des recherches of the University Henri Poincaré Nancy, 2000.